# *sizzled* function and secreted factor network dynamics

**Jianli Shi[1], Huarong Zhang[1], Robin D. Dowell[2] and Michael W. Klymkowsky[1,*]**

[1]Molecular, Cellular and Developmental Biology, University of Colorado, Boulder, CO 80309-0347, USA
[2]BioFrontiers, University of Colorado, Boulder, CO 80309-0347, USA
*Author for correspondence (michael.klymkowsky@colorado.edu)

*Biology Open* 1, 286–294
doi: 10.1242/bio.2012019

## Summary

**Studies on the role of the E-box binding transcription factor Snail2 (Slug) in the induction of neural crest by mesoderm (Shi et al., 2011) revealed an unexpected increase in the level of *sizzled* RNA in the dorsolateral mesodermal zone (DMLZ) of morphant *Xenopus* embryos. *sizzled* encodes a secreted protein with both Wnt and BMP inhibitor activities. Morpholino-mediated down-regulation of *sizzled* expression in one cell of two cell embryos or the C2/C3 blastomeres of 32-cell embryos, which give rise to the DLMZ, revealed decreased expression of the mesodermal marker *brachyury* and subsequent defects in neural crest induction, pronephros formation, and muscle patterning. Loss of *sizzled* expression led to decreases in RNAs encoding the secreted Wnt inhibitor SFRP2 and the secreted BMP inhibitor Noggin; the *sizzled* morphant phenotype could be rescued by co-injection of RNAs encoding Noggin and either SFRP2 or Dickkopf (a mechanistically distinct Wnt inhibitor). Together, these observations reveal that *sizzled,* in addition to its established role in dorsal-ventral patterning, is also part of a dynamic BMP and Wnt signaling network involved in both mesodermal patterning and neural crest induction.**



Key words: sizzled, Secreted signaling antagonists, WNT, BMP, Neural crest induction, Signaling networks



## Introduction

A large number of secreted signaling agonists are expressed in the early *Xenopus* embryo, including Wnts, BMPs, Nodals, and FGFs together with their antagonists (De Robertis, 2009; De Robertis and Kuroda, 2004; Schier, 2009; Smith, 2009). One component of the early embryo's extracellular signaling system is Sizzled, a secreted protein with homology to the extracellular domain of the Wnt receptor Frizzled (Collavin and Kirschner, 2003; Salic et al., 1997). Previous studies reported that *sizzled* expression is regulated by, and regulates BMP signaling (Lee et al., 2006; Muraoka et al., 2006) and that Sizzled "functions in a negative feedback loop that limits allocation of mesodermal cells to the extreme ventral fate" (Collavin and Kirschner, 2003). Our interest in *sizzled* was spurred by the observation that *sizzled* RNA levels in the dorsolateral mesoderm increased in response to blocking the expression of the transcription factor Snail2/Slug, an important regulator of both mesoderm and neural crest differentiation in *Xenopus* (Shi et al., 2011).

Sizzled was originally identified by Salic et al., as a Wnt inhibitor. Its expression begins in the ectodermal (animal cap) region at the midblastula transition (stage 8.5), subsequently its expression becomes restricted to the ventral marginal zone (VLZ) and ventral animal cap (Salic et al., 1997). In retrospect, the complexity of Sizzled's function is not surprising. Sizzled is a member of the family of "secreted frizzled receptor-like proteins" (SFRPs) (Bovolenta et al., 2008; Esteve and Bovolenta, 2010). In addition to binding to and inhibiting Wnt signaling, SFRPs have been found to bind to Frizzleds directly, or in a complex with Wnts, thereby activating Wnt signaling. They can enhance Wnt diffusion (Mii and Taira, 2009) and have been found to bind other proteins, such as RANKL, blocking its ability to activate NF-κB signaling through the RANK receptor (Hausler et al., 2004). NF-κB is involved in the patterning of the early *Xenopus* embryo (Beck et al., 1998; Kennedy et al., 2007; Kennedy and Kao, 2011; Lake et al., 2001; Tannahill and Wardle, 1995; Zhang et al., 2006). Perhaps more surprisingly, first Sizzled and then the related protein Crescent were found to act indirectly as BMP inhibitors by binding to, and inhibiting the activity of secreted Tolloid-like/BMP1-like metalloproteinases, which in turn inhibit the BMP inhibitor Chordin (Lee et al., 2006; Misra and Matise, 2010; Muraoka et al., 2006; Ploper et al., 2011; Yabe et al., 2003). Subsequently it was found that the related protein, SFRP2, binds to and activates Tolloid-like proteins, such as procollagen C proteinase (Kobayashi et al., 2009), raising the prospect of complex positive and negative interactions between SFRPs and secreted enzymes.

We originally set out to test the hypothesis that blocking the increase in *sizzled* RNA found in Snail2/Slug morphant embryos would rescue the Snail2/Slug morphant phenotype. This experiment was complicated by the fact that blocking *sizzled* expression itself produce both mesodermal and neural crest phenotypes, which we show can be rescued by the injection of RNAs encoding BMP and Wnt antagonists, suggesting that Sizzled normally acts, either directly or indirectly, as both a BMP and a Wnt inhibitor.

## Results

Expression of *sizzled* RNA begins following the midblastula transition (stage 8.5) in the animal (ectodermal) region, before becoming restricted to the ventral regions of gastrula stage embryos (Salic et al., 1997). In our hands whole-mount *in situ* hybridization (Fig. 1A–E), standard (Fig. 1F) and quantitative

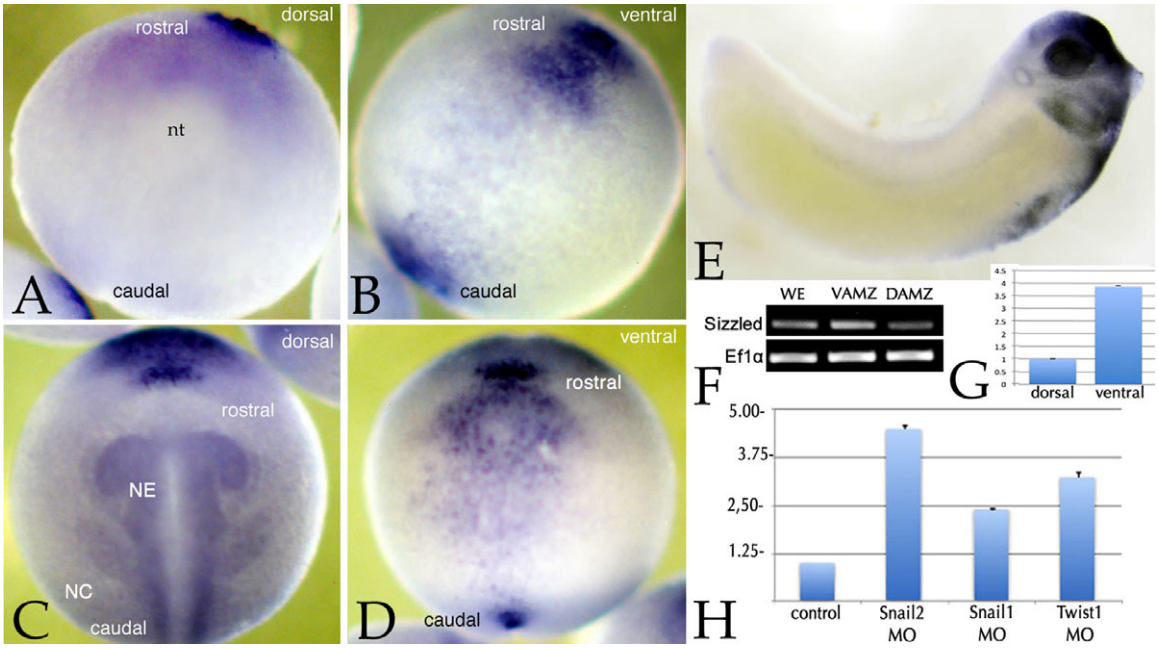


**Fig. 1. Expression analysis of *sizzled*.** *In situ* hybridization of stage 12 **(A,B)** and stage 18 **(C,D)** embryos revealed high levels of expression in both rostral and caudal ventral regions, as well as lower, but detectable expression within the neural ectoderm and neural crest. In later stages, *sizzled* in situ hybridization staining **(E)** was readily detected in the ventral and cranial regions. Standard RT-PCR **(F)** (stage 11) revealed readily detectable levels of *sizzled* RNA in whole embryos (WE), the ventral axial marginal zone (VAMZ) and dorsal axial marginal zone (DAMZ). Quantitative RT-PCR of the dorsal and ventral regions of stage 25 embryos **(G)** revealed readily detectable levels of *sizzled* RNA in both regions. qPCR analysis **(H)** of control and morpholino-injected embryos (both blastomeres of 2 cell embryos injected, embryos analyzed at stage 11) reveal an increase in *sizzled* RNA *snail2/slug*, *snail1*, and *twist1* morphant embryos.

RT-PCR (*q*PCR) studies (Fig. 1G) revealed detectable levels of *sizzled* RNA in both ventral and dorsal axial marginal zones of early gastrula stage embryos, as well as in the dorsal region of early neurula stage embryos. *q*PCR analysis of whole embryos (Fig. 1H) confirmed that *sizzled* RNA levels increased in *snail2*, *snail1*, and *twist1* morphant gastrula (stage 11.5) embryos (both cells of two cell stage embryos injected). In RNA SEQ of whole *snail2* morphant *Xenopus tropicalis* embryos (Table 1), *sizzled* RNA levels were increased ~3 fold compared to control morpholino injected embryos (analyzed at stage 11.)

Given the increase in *sizzled* RNA levels in *snail2* C2/C3 morphant DLMZs found previously (Shi et al., 2011), we were interested in answering the question, does blocking the increase in *sizzled* expression (through morpholino injection) rescue the *snail2* morphant phenotype? As describe below, this goal was complicated by the fact that i) loss of *snail2* activity also leads to an increase in RNA levels for two other secreted signaling antagonists, *cerberus* and *chordin* (Shi et al., 2011; Zhang and Klymkowsky, 2009), and ii) the observation that *sizzled* has its own role within the DLMZ with respect to mesodermal and neural crest differentiation. Since we have yet to identify a useful anti-*Xenopus* Sizzled antibody, we tested the efficacy of the *sizzled* morpholino by co-injecting embryos with RNAs (200 pg/embryo) encoding GFP and Sizzled-HA or a similarly epitope-tagged form of a mutated and inactive form of Sizzled, SizzledD92W-HA (Lee et al., 2006). Both RNAs contain the morpholino's target sequence; in both cases, the morpholino (injected at 7 ngs/embryo) significantly reduced, but did not eliminate the accumulation of the exogenous polypeptide (Fig. 2A). Similar results were observed when an RNA encoding a GFP-tagged form of Sizzled was injected; the *sizzled* morpholino dramatically reduced fluorescence, while injection of control morpholino had no effect on Sizzled-HA/GFP accumulation (data not shown). Since the level of injected RNA is estimated to be greater than the level of endogenous *sizzled* RNA, we expect that the *sizzled* morpholino will produce a fairly robust hypomorphic (reduction of function) phenotype. We also note that the amount of morpholino used in these and all other studies (7 ngs/embryo) is at the low end of that commonly used, which has been reported to be as high as 40 to 60 ngs/embryo.

**Table 1. Data from snail2 morphant RNA SEQ analysis in *X. tropicalis*.**

| *snail2 MO* | *control MO* | *significance* | *sizzled (snail MO) / sizzled (control MO)* |
|---|---|---|---|
| 94.4 | 31.3 | 6.00 E-15 | 3.02 |

We first characterized *sizzled* morpholino "half-embryo" effects; in such studies the morpholino was injected equatorially into one cell of a two-cell embryo (Table 2). In gastrula stage embryos, we found loss of expression of the mesodermal marker *brachyury* (Fig. 2B,C) and increased expression of the endodermal marker *endodermin* (Fig. 2E,F). Both could be rescued by injection of 200 pgs sizzled-HA RNA (Fig. 2D,G); higher levels of RNA produced their own effects (see below.) In later stage embryos, we found disruption of pronephric development (Fig. 2H,H*) and myotomal organization (Fig. 2I–N) on the morphant sides of embryos.

Previously we found that *snail2* morpholino injection of the C2/C3 blastomeres of the 32-cell embryo led to a loss of mesoderm and neural crest, while *snail1* and *twist1* morphant, C2/C3 injected embryos lost mesoderm but not neural crest (Shi et al., 2011). When the *sizzled* morpholino was injected into C2/C3 blastomeres we found the loss of *xbra* expression in early

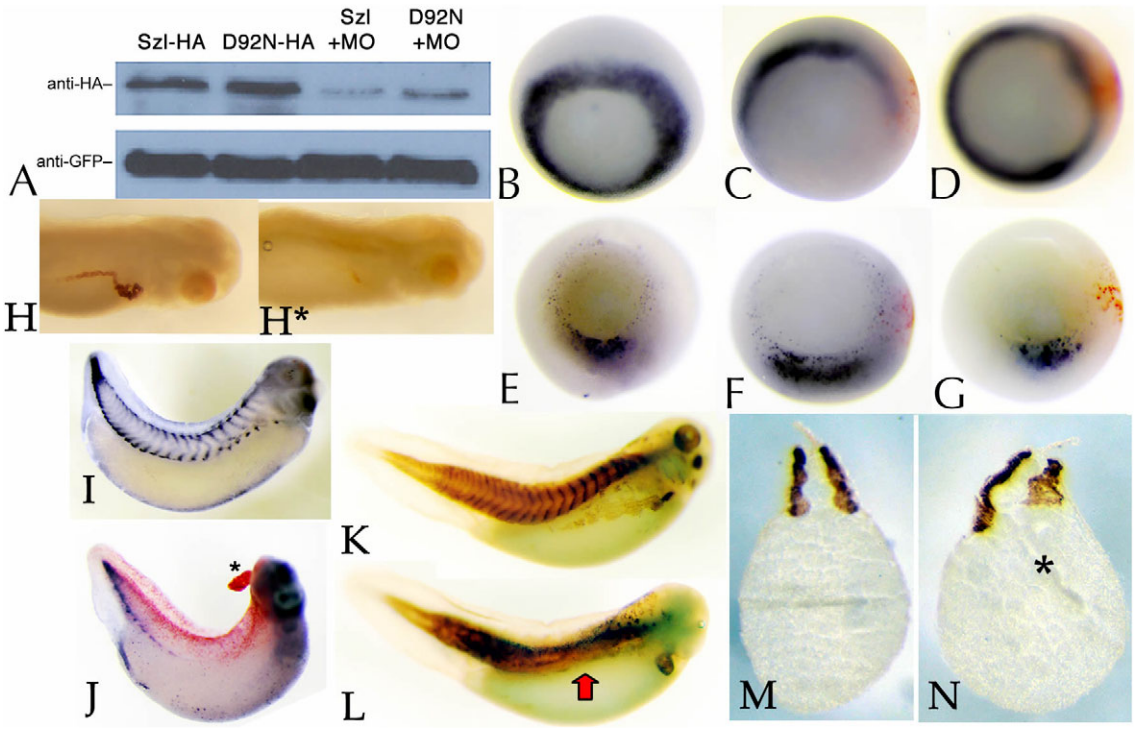


**Fig. 2. Morpholino-based studies of *sizzled* function. (A)** 1 cell embryos were injected with RNA encoding either Sizzled-HA or SizzledD92N-HA (200 pgs/embryo) together with 200 pgs/embryo GFP RNA either alone or together with 7 ngs/embryo *sizzled* morpholino; immunoblot analysis of stage 11 embryos indicated that GFP accumulation was unaffected by morpholino injection, while Sizzled-HA protein levels were reduced, but not completely eliminated. Injection of the *sizzled* morpholino into 1 cell of 2 cell embryos, together with RNA encoding lacZ as a lineage marker, revealed that compared to control embryos **(B)**, there was a decrease in *xbra* in situ hybridization staining **(C)** that could be rescued by the co-injection of *sizzled* RNA **(D)**. Similarly, the expression of the endodermal marker *endodermin* **(E)** was increased in *sizzled* morphant embryos **(F)**, and this increase was reversed by *sizzled* RNA injection **(G)**. These effects extended into later stages. Staining with the monoclonal antibody 4A6, which labels the pronephros, revealed a decrease in staining on the injected **(H*)** compared to the uninjected sides **(H)** of stage 30 embryos. Similarly, the expression of *myoD* (**(I)**-control, **(J)**-*sizzled* morpholino) (* indicates injection artifact) and the organization of somatic myotomal muscle, visualized by whole-mount staining with an antibody against tropomyosin, (**(K)**, **(M)**-control, **(L)**-*sizzled* morpholino-injected side, **(N)**-section of whole-mount stained, injected embryo) were disrupted in sizzled morpholino injected regions of the embryo (* indicates injected side in part N).

gastrula stage embryos (Fig. 3A–C), loss of the neural crest markers *snail2* (Fig. 3D–F), *twist1* (Fig. 3G–I) and *sox9* (Fig. 3J–L) as well as the loss of *myoD* expression (Fig. 3M,O) in later stage embryos (Table 3). The sizzled morpholino effect on sox9 expression was efficiently rescued by the injection of the *sizzled* RNA but not by injection of *sizzled* D92N RNA (Fig. 3O). An interesting observation was that while *sizzled* morpholino injection led to a "simple" reduction of the *snail2* and *sox9* expression domains, its effects on *twist1* expression were more complex, with both reduced and apparently ectopic ectodermal expression observed (Fig. 3I).

Because the C2/C3 lineage gives rise to a range of tissues (Dale and Slack, 1987; Moody, 1987; Nakamura et al., 1978), we examined whether the effects on ectodermal neural crest marker expression were due to inductive (secreted factor-mediated) effects by using a standard explant sandwich approach (Bonstein et al., 1998; Shi et al., 2011). When wild type ectoderm (animal cap) is cultured alone it remains undifferentiated epidermis (Fig. 4A); when cultured with wild type DLMZ, the animal cap expresses neural crest markers, such as *sox9* (Fig. 4B). We found that DLMZ from *sizzled* morpholino-C2/C3 injected embryos produced a much weaker inductive effect in terms of *sox9* expression (Fig. 4C). Quantitative RT-PCR analysis of explants (Fig. 4D) supported this conclusion; the increases in *sox9*, *snail2*, and *twist1* RNA levels observed in wild type animal cap/wild type DLMZ explants were reduced to below the levels observed in wild type animal caps alone in wild type animal cap/sizzled morphant DLMZ explants. This indicates that loss of *sizzled* function leads to a loss of inductive activity, as well as other negative effects on *sox9*, *snail2*, and *twist1* expression in this system.

BMP and Wnt signaling have been implicated in mesodermal induction of neural crest (see Shi et al., 2011 and references therein). To examine the signaling system influenced by *sizzled* loss of function, we took three approaches. First, we isolated DLMZ from *sizzled* morphant, C2/C3 injected embryos and subjected them to *q*PCR analysis. The result shows a small but reproducible increase in the levels of *wnt8* and *bmp4* RNAs and more dramatic decreases in the levels of *noggin* and *sfrp2* RNAs

**Table 2. *sizzled* morphant embryos (1/2 injection) analysed at stage 18.**

| | Total No. | Normal | Mild phenotype | Moderate phenotype | Severe phenotype |
|---|---|---|---|---|---|
| Xbra | 40 | 40% | 20% | 20% | 20% |
| MyoD | 50 | 12% | 8% | 24% | 56% |
| Edd | 32 | 19% | 31% | 31% | 19% |
| Sox9 | 30 | 13% | 23% | 50% | 14% |
| Snail2/Slug | 30 | 20% | 27% | 26% | 27% |
| Twist | 39 | 15% | 26% | 38% | 21% |

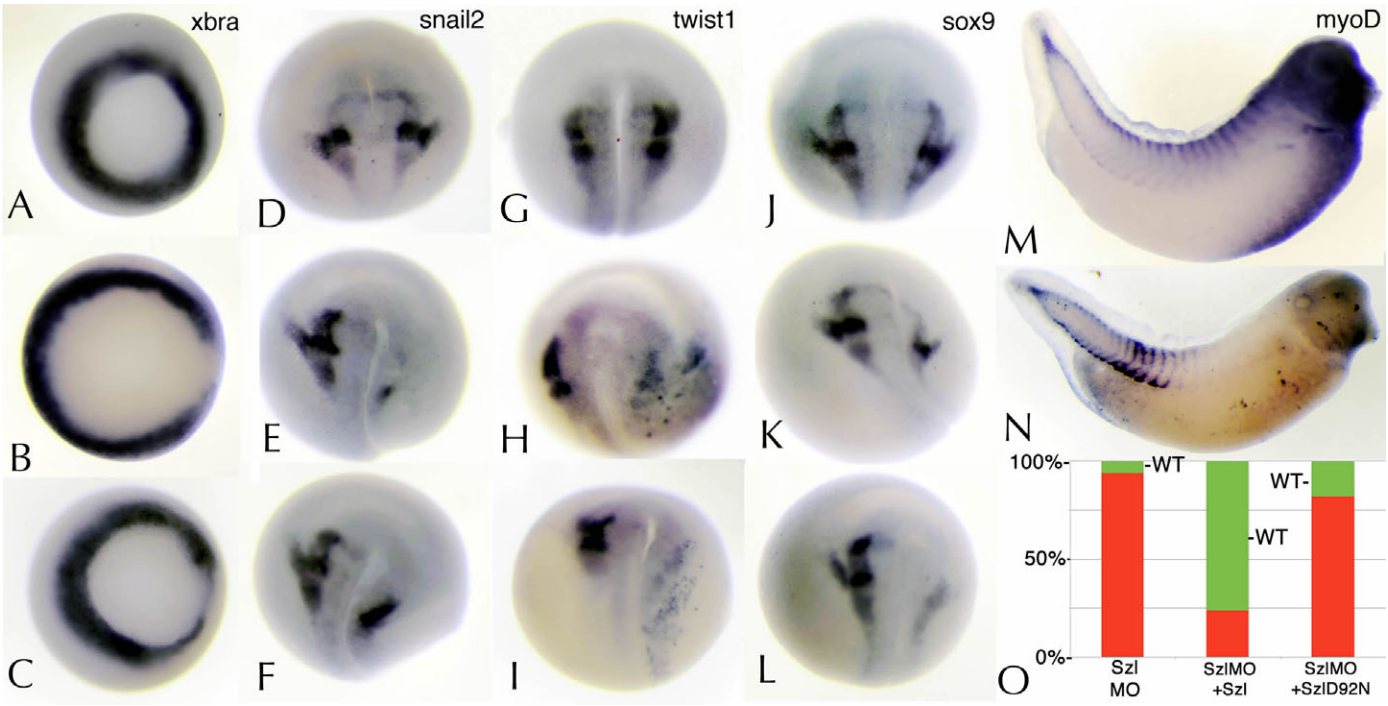


**Fig. 3. 32-cell sizzled morphant phenotypes and rescue.** *Sizzled* morpholino was injected, together with GFP RNA, into the C2/C3 blastomeres of 32 cell stage embryos. Embryos were sorted based on fluorescence at stage 10. Stage 11 embryos were stained for *xbra* RNA (**(A)**-control, **(B,C)**-morphant); stage 18 embryos were stained for *snail2* (**(D)**-control, **(E,F)**-morphant), *twist1* (**(G)**-control, (**H,I)**-morphant), *sox9* (**(J)**-control, **(K,L)**-morphant) RNAs. Effects on *myoD* RNA were examined at stage 25 (**(M)**-control, **(N)**-morphant). **(O)** *sox9* expression in *sizzled* MO embryos was rescued by *sizzled* RNA injection (200 pgs/embryo) but not by *sizzled* D92N RNA (green bars indicate percentage of embryos with a wild type phenotype, red bars indicate loss of *sox9* RNA staining).

**Table 3. sizzled morphant embryos (C2C3 injection), analyzed at stage 18.**

| | Total No. | Normal | Mild phenotype | Moderate phenotype | Severe phenotype |
|---|---|---|---|---|---|
| Xbra | 45 | 27% | 36% | 24% | 13% |
| MyoD | 40 | 20% | 20% | 20% | 40% |
| Sox9 | 40 | 26% | 20% | 27% | 27% |
| Slug | 20 | 40% | 50% | 10% | 0 |
| Twist | 20 | 25% | 65% | 10% | 0 |

(Fig. 5A). Levels of *dkk*, *frzb1*, and *chordin* RNAs appeared unchanged. We then asked whether the C2/C3 *sizzled* morphant phenotype could be rescued by injection of *noggin* or *sfrp2* RNAs, either alone or together. Alone, neither *noggin* or *sfrp2* RNAs rescued the C2C3 sizzled morphant phenotype, but together rescue was robust (Fig. 5B). Since SFRP2 interacts with tolloid-like proteins (Kobayashi et al., 2009), it is possible that it has both anti-Wnt and (indirect) anti-BMP activities. We therefore repeated these studies using RNAs encoding Noggin and the Wnt antagonist Dickkopf (Dkk), which acts in a distinctly different mechanism from SFRPs (Bafico et al., 2001; Semenov et al., 2001). Again, we found that only the combination of the BMP inhibitor Noggin and the Wnt antagonist Dkk efficiently rescued the *sizzled* morphant phenotype (Fig. 5C), suggesting that both signaling pathways are involved, and that the Wnt/BMP signaling balance is important in neural crest induction by

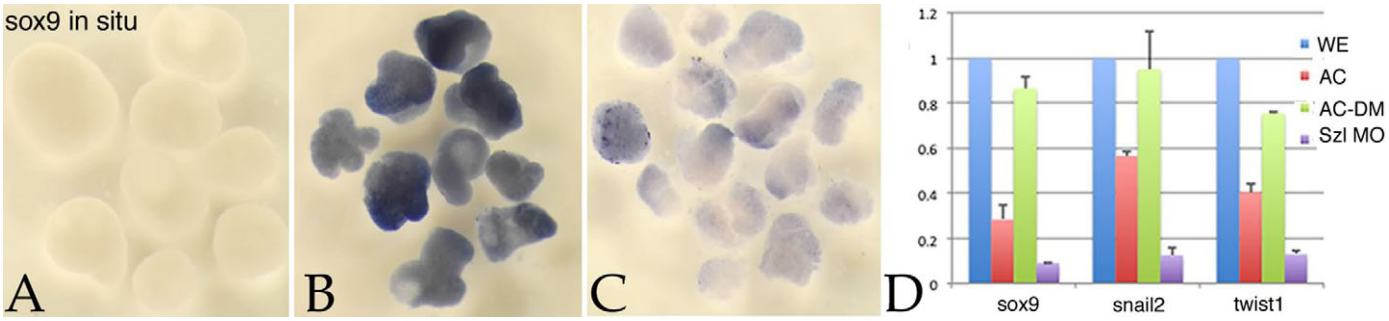


**Fig. 4. Sizzled-dependent induction in ectodermal-DLMZ explants.** Ectodermal explants were isolated from stage 8/9 embryos and cultured either alone **(A)** or together with DLMZ explants, isolated from stage 10 wild type **(B)** or *sizzled* C2/C3 morphant **(C)** embryos. When control embryos reached stage 18, explants were stained in situ for *sox9* RNA. In similar studies **(D)**, explants were analyzed when control embryos reached stage 11 by qPCR for levels of *sox9*, *snail2*, or *twist1* RNAs. Levels of these RNAs in whole embryos (WE), animal caps (AC), control animal cap-dorsal mesoderm (AC-DM) or control animal cap-sizzled morphant dorsal mesoderm (*sizzled* MO) were compared.

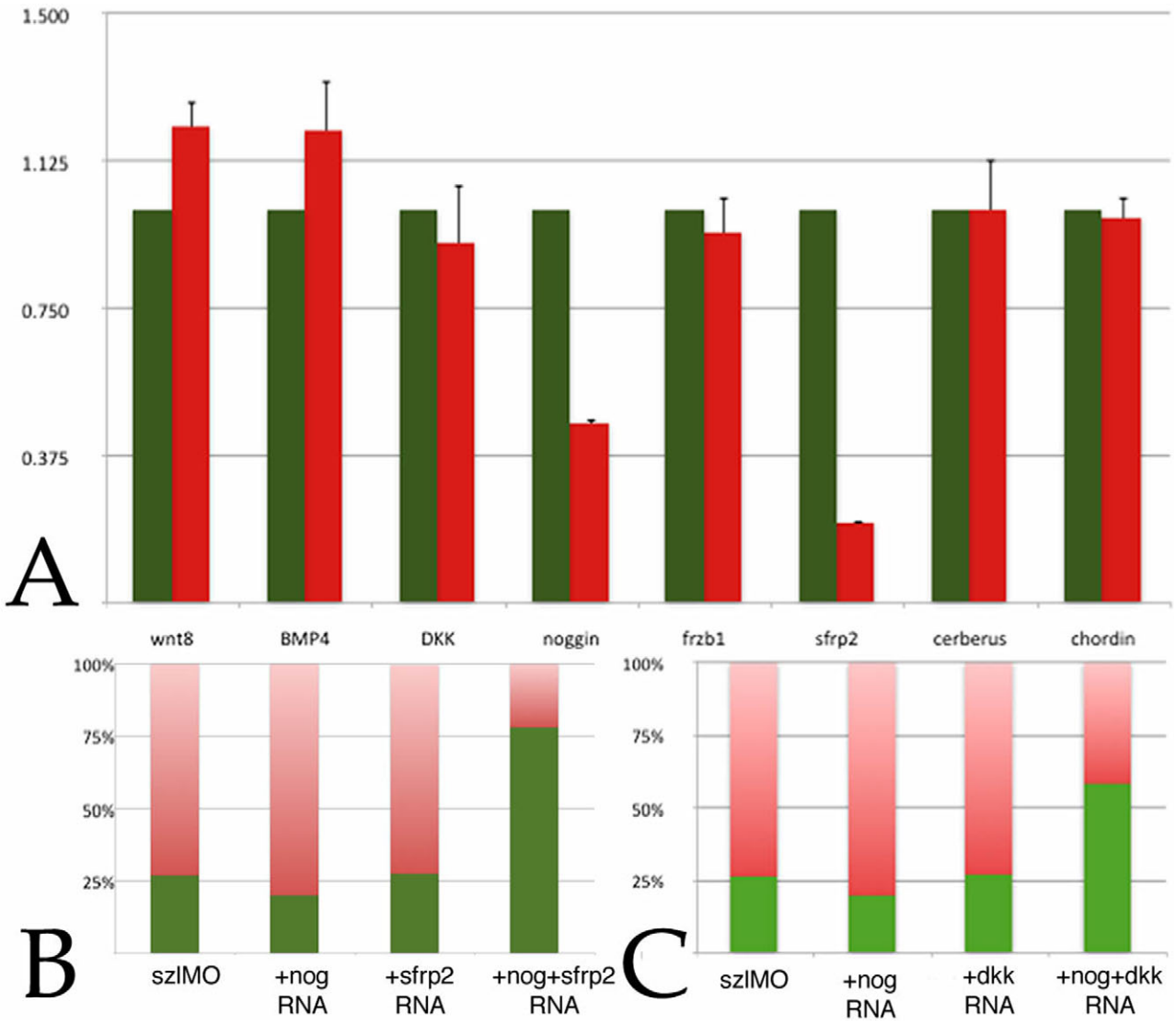


**Fig. 5. Sizzled-dependent changes in DLMZ gene expression and antagonist rescue studies. (A)** The DLMZ region (at stage 11) was isolated from C2/C3 *sizzled* morphant embryos and subjected to qPCR analysis. Compared to control DLMZs (green), *sizzled* morphant DLMZs (red) showed small but reproducible increases in *wnt8* and *bmp4* RNA levels, and reproducible decreases in *noggin* and and *sfrp2* RNA levels. **(B)** We then examined the ability of injection of *noggin* and *sfrp2* RNAs, either alone or together, to rescue the *sizzled* C2/C3 morphant *sox9* phenotype: neither was effective alone, but in combination they produced a robust rescue. Green bars indicated rescued embryos, red bars indicate loss of sox9 expression. **(C)** Given that SFRP2 may have both anti-Wnt and anti-BMP activities, we examined the behavior of the "pure" Wnt antagonist Dkk. As before, neither *noggin* or *dkk* RNAs alone rescued, but together they produced a greater than 50% rescue of *sox9* expression.

DLMZ-derived factors. This supports our previous conclusion (Shi et al., 2011), that both signaling systems are involved in mesodermal induction of neural crest.

### Over-expression studies

In the course of experiments to rescue the *sizzled* morphant phenotype using *sizzled* RNA injection, we noted a dramatic dose response. At low RNA levels (~200 pgs/embryo), the levels used to rescue *sizzled* morphant phenotypes, the effects of *sizzled* RNA injection were relatively subtle–as an example, we found increases in levels of *sox9* (Fig. 6A,B) and *twist1* (Fig. 6D,E) expression on the injected side of neurula (stage 18) embryos. In contrast moderately higher levels (~600 pgs/embryo) led to dramatic effects on both injected and contralateral sides of the embryo in terms of *sox9* (Fig. 6C), *twist1* (Fig. 6F), *snail2* (Fig. 6G,H), *chd7* (Fig. 6I), and *c-myc* (Fig. 6J–L), reinforcing the general caution associated with interpreting over-expression studies, particularly with regards to secreted proteins and in systems that display dramatic adaptive behavior (De Robertis, 2009), as illustrated by the changes in *noggin* and *sfrp2* RNA levels seen in *sizzled* morphant embryos.

### Whole embryo RNA SEQ studies in *X. tropicalis*

Because the *X. tropicalis* genome sequence is available (Hellsten et al., 2010), while that of *X. laevis* is not, we carried out an RNA SEQ analysis of *sizzled* morphant *X. tropicalis* embryos. Both blastomeres of two cell embryos were injected with 7 ngs/embryo control or *sizzled* morpholino. RNA was isolated when control embryos reached stage 11. Our analysis identified ~700 RNAs whose levels were changed in sizzled *morphant* embryos

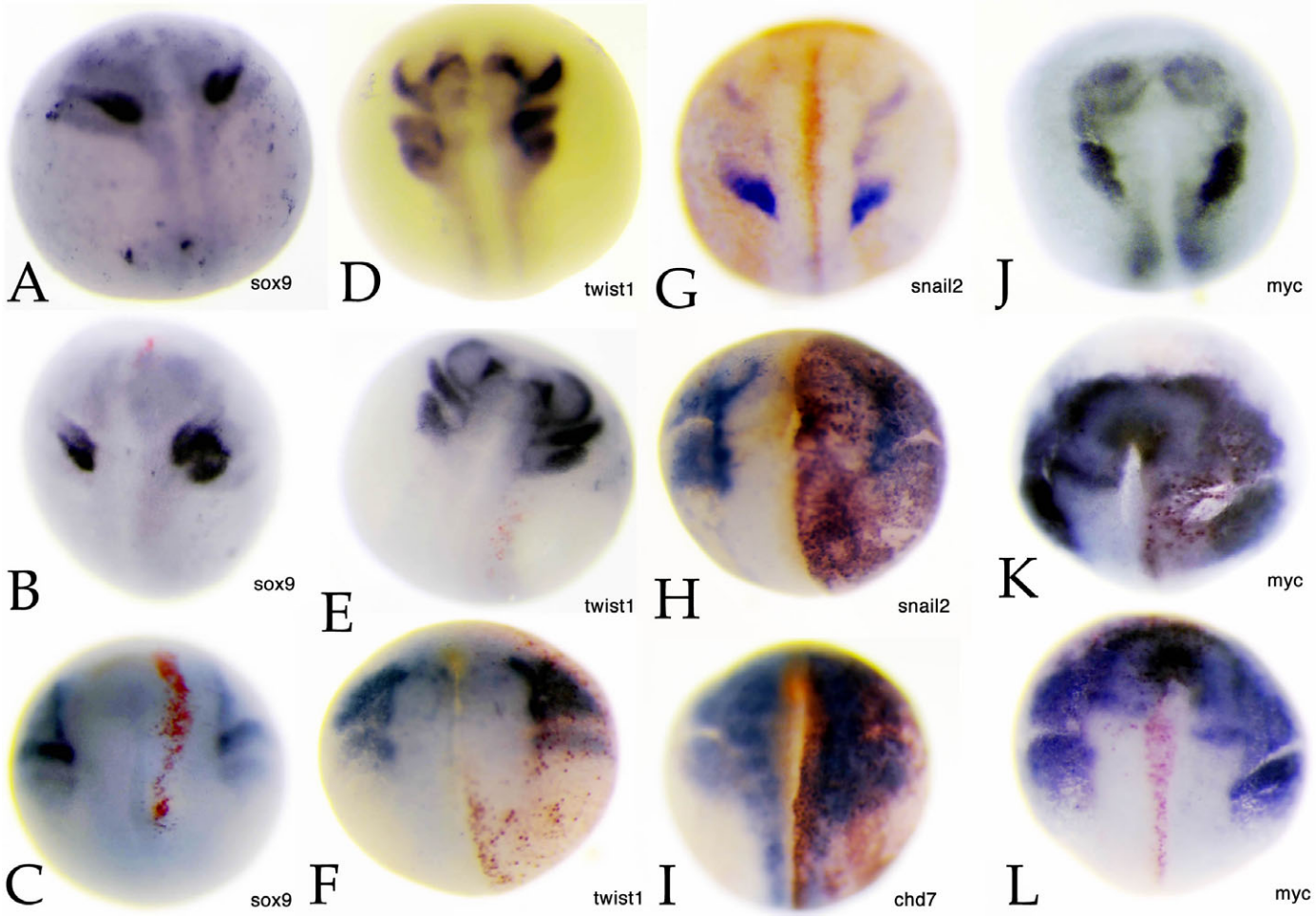


**Fig. 6. Effects of sizzled over-expression.** The effects of *sizzled* over-expression were complex, as illustrated when the effects of injecting low (200 pgs/embryo) or high (600 pgs/embryo) amounts of *sizzled-HA* RNA into one blastomere of two cell embryos (control, uninjected side to the left in all images.) At stage 18, the effects on the expression of *sox9* (**(A)**-control, **(B)**-low, **(C)**-high) and *twist1* (**(D)**-control, **(E)**-low, **(F)**-high), *snail2* (**(G)**-control, **(H)**-high), *chd7* (**(I)**-high), and *c-myc* (**(J)**-control, **(K,L)**-high) were analyzed. In embryos injected with 200 pgs of Sizzled-HA RNA the *sox9* expression domain was altered in 27 of 30 embryos (B); the *twist1* expression domain was altered in 26 of 31 embryos (E); the *snail2* expression domain was altered in 26 of 30 embryos (G); and the *chd7* expression domain was altered in 19 of 24 embryos (data not shown). In embryos injected with 600 pgs of Sizzled-HA RNA, the *sox9* expression domain was altered in 21 of 24 embryos (C); the *twist1* expression domain was altered in 19 of 22 embryos (F); the *snail2* expression domain was altered in 22 of 26 embryos (H); the *chd7* expression domain was altered in 16 of 18 embryos (I); and the *c-myc* expression domain was altered in 24 of 28 embryos (K,L). Red-brown staining indicates lacZ staining due to co-injected LacZ RNA (used as a lineage marker).

compared to controls (p values$<$0.002) (supplementary material Sizzled morphant, X. tropicalis RNA SEQ data – Excel file). While it is clear that targeted regional and perturbation studies, which we plan to carry out in *X. laevis* once its genome sequence is available, are required to make sense of these data, we do note that a number of genes encoding transcription factors associated with mesodermal and muscle differentiation, as well as genes encoding secreted factors are altered (Table 4).

## Discussion

The role of Sizzled in dorsal-ventral axis formation is well established (Collavin and Kirschner, 2003). Here we demonstrate that *sizzled* also plays a role within the DLMZ, where its loss of function leads to a range of down-stream effects, including disrupting neural crest, as well as pronephros and somatic muscle formation, both mesenchymal tissues (Kielbowna, 1981; Muntz, 1975; Wessely and Tran, 2011). While there has been some confusion about whether Sizzled acts as a Wnt inhibitor (Salic et al., 1997) or an indirect BMP inhibitor (through the sizzled tolloid ⊣ chordin ⊣ BMP ⊣ pathway) (Lee et al., 2006; Muraoka et al., 2006), our studies suggest that it plays both roles in the DLMZ; that said, it is not clear whether its ability to inhibit Wnt signaling is direct (e.g. by binding to Wnts) or indirect (in analogy to its ability to inhibit BMP signaling.) Moreover, it is likely that the phenotypic effects observed in *sizzled* C2/C3 morphant embryos represent the end result of a cascade of effects, in which changes in *noggin* and *sfrp2*, along with other genes (altered in response to *sizzled* loss of function) play an important role, linked in part to more general effects on BMP and Wnt signaling.

What is clear is that SFRP family proteins, like Sizzled, have more complex functions than originally expected. Our RNA SEQ studies in *X. tropicalis* suggest they may well be involved in regulating the levels of RNAs encoding a number of secreted factors (Table 4) including a number of ADAM and matrix metalloproteinases. While we are currently in the process of confirming the regional effects of *sizzled* loss of function in *X. laevis*, as well as the role of particular Sizzled-regulated target genes in axial patterning and mesodermal and neural crest

**Table 4. Transcription and secreted factor encoding RNAs altered in *sizzled* (2/2) morphant *X. tropicalis* embryos (analyzed at stage 11).**

| gene | Sizzle MO* | Control MO* | ln fold change | p value | | gene name |
|---|---|---|---|---|---|---|
| myod1 | 1.77 | 13.4 | 2.02 | 3.32E-11 | down ↓ | myoD1 |
| myos | 1.50741 | 5.14 | 1.23 | 1.07E-09 | down ↓ | myoskeletin |
| msgn1 | 21.4913 | 58.3 | 0.998 | 1.34E-06 | down ↓ | mesogenin 1 (paraxial mesoderm) |
| sox5 | 0.0907083 | 1.12 | 2.51 | 4.13E-06 | down ↓ | sox5 (hypaxial muscle) |
| meox2 | 1.41143 | 4.93 | 1.25 | 7.06E-06 | down ↓ | mesenchyme homeobox 2 |
| myf5 | 40.8759 | 92.9 | 0.821 | 1.11E-05 | down ↓ | myogenic factor 5 |
| twist1 | 7.81983 | 19.4 | 0.909 | 9.38E-05 | down ↓ | twist1 |
| foxc2 | 27.8 | 51.3 | 0.615 | 0.0007 | down ↓ | forkhead box C2 |
| gsc | 66.0 | 9 | −0.667 | 0.0004 | up ↑ | goosecoid<br>↑ transcription factors ↑<br>↓ secreted/membrane proteins ↓ |
| nodal3 | 15.3 | 3.14 | −1.58365 | 2.15E-10 | up ↑ | nodal3 |
| nodal6 | 2.79 | 0.963 | −1.06483 | 0.0009 | up ↑ | nodal homolog 6 |
| nodal1 | 7.29671 | 3.2317 | −0.814415 | 0.002 | up ↑ | nodal1 |
| sod3 | 1.23974 | 0.178928 | −1.94 | 0.002 | up ↑ | superoxide dismutase 3, extracellular [*] |
| adamts3 | 3.82516 | 1.264 | −1.10732 | 1.45E-05 | up ↑ | ADAM metallopeptidase |
| cxcr4 | 80.8664 | 44.6908 | −0.593031 | 0.00093 | up ↑ | chemokine (C-X-C motif) receptor 4 |
| gdf1 | 21.9362 | 10.9589 | −0.693985 | 0.001 | up ↑ | growth differentiation factor 1 |
| adam9 | 0.228815 | 0 | −1.80E+308 | 0.001 | up ↑ | ADAM metallopeptidase domain 9 |
| mmp21 | 0.0356713 | 0.67296 | 2.93734 | 7.88E-05 | down ↓ | matrix metallopeptidase 21 |
| kcp | 0.0811106 | 0.475896 | 1.76939 | 8.83E-05 | down ↓ | kielin/chordin-like protein |
| fgfbp3 | 0.576005 | 1.99487 | 1.24222 | 0.000142 | down ↓ | fibroblast growth factor binding protein 3 |
| darmin | 149.943 | 292.273 | 0.667432 | 0.00067 | down ↓ | darmin (secreted endodermal factor) |
| mmp3 | 4.86047 | 15.5079 | 1.16022 | 3.90E-07 | down ↓ | matrix metallopeptidase 3 |
| kremen2 | 0.138835 | 1.4752 | 2.36326 | 2.07E-06 | down ↓ | Dkk receptor |
| fstl1 | 1.27655 | 4.86586 | 1.33808 | 3.68E-06 | down ↓ | follistatin-like 1 |
| socs3 | 2.08572 | 4.82826 | 0.84 | 0.002 | down ↓ | suppressor of cytokine signaling 3 |
| mmp3 | 4.86047 | 15.5079 | 1.16022 | 3.90E-07 | down ↓ | matrix metallopeptidase 3 |
| dhh | 1.30183 | 2.99325 | 0.832589 | 0.001 | down ↓ | desert hedgehog |
| adamts18 | 0.237937 | 0.640677 | 0.99 | 0.002 | down ↓ | ADAM metallopeptidase |

*Complete dataset supplied in supplementary material Table S1.

differentiation, the broader significance of these observations involves the linkage between *snail2/slug*, a gene well known to be involved in tumor metastasis (Alves et al., 2009; Hanahan and Weinberg, 2011; Hugo et al., 2011; Micalizzi et al., 2010; Shirley et al., 2010), and metastatic behavior (Klymkowsky and Savagner, 2009). There is increasing evidence for the importance of secreted factor mediated tumor-stroma interactions (Chaffer and Weinberg, 2011; Hanahan and Weinberg, 2011), and it seems plausible that Sizzled is part of a network of interactions that regulates how cells interact with their extracellular environment.

## Materials & Methods

### Embryos and their manipulation

*X. laevis* embryos were staged, and explants and co-explants were generated following standard procedures (Klymkowsky and Hanken, 1991; Nieuwkoop and Faber, 1967; Sive et al., 2000; Zhang et al., 2003). Similar studies were carried out using *X. tropicalis* embryos following methods posted on the Harland (http://tropicalis.berkeley.edu/home/) and Khokha (http://tropicalis.yale.edu/) lab web sites, using animals purchased from Xenopus I. Capped mRNAs were transcribed from linearized plasmid templates using mMessage mMachine kits (Ambion) following manufacturer's instructions. For two-cell stage studies, embryos were injected equatorially; for 32-cell stage studies, C2 and C3 blastomeres were routinely co-injected with RNA encoding GFP and examined at stage 10 to confirm the accuracy of injection. Animal caps were isolated from stage 8–9 blastula embryos in 0.5 MMR (Sive et al., 2000) transferred into wells of an 2% agarose plate (one animal cap per well) and combined with DLMZ isolated from stage 10.5 gastrula embryos according to Bonstein et al. (Bonstein et al., 1998). Explant recombinants were harvested when siblings reached stage 18. Images were captured using either a Nikon CoolPix 995 Camera on a Leica M400 Photomicroskop or a Nikon D5000 camera on a Wild stereomicroscope. Images were manipulated with Fireworks CS4 software (Adobe) using "auto levels", "curves" and "levels" functions only.

### Morpholinos and plasmids

For this study, morpholinos against *snail2*, *snail1*, and *twist1* RNA are as described previously (Shi et al., 2011; Zhang et al., 2006; Zhang and Klymkowsky, 2009). The *snail2* morpholino matches the *X. tropicalis snail2* sequence at 24 of 25 positions. We generated a new morpholino, designed by Gene Tools, Inc (5′ AGAGGAGCAGGAAGACTCCGGACAT 3′) to block the translation of *X. laevis sizzled* RNA. This sizzled morpholino matches the *X. tropicalis* sizzled RNA at 19 consecutive bases, with two mismatches (out of 25). Plasmids encoding HA-tagged forms of Sizzled were supplied by Eddy DeRobertis (UCLA); we constructed a plasmid encoding sizzled-GFP using the pCS2mt-GFP plasmid (Rubenstein et al., 1997). RNA injected embryos were selected based on GFP-based fluorescence. Eddy DeRobertis and Richard Harland supplied plasmids encoding Sizzled (Salic et al., 1997), Noggin (Smith and Harland, 1992), and Dickkopf (Glinka et al., 1998).

### RNA SEQ analysis in *X. tropicalis*

RNA SEQ was carried out on a next-generation Illumina HiSeq instrument, part of the Colorado Institute for Molecular

Biotechnology facility run by Dr Jim Huntley. Standard Trizol and Qiagen RNeasy methods (Akkers et al., 2009) were used to isolate total RNA from stage 11 control and *sizzled* morphant embryos (injected in both blastomeres of the two cell stage.) Poly-adenylated mRNA was selected using a polyA Spin mRNA Isolation Kit (NEB). 4 µg RNA was taken into each mRNA-SEQ library preparation. Indexed mRNA-SEQ libraries were prepared using Illumina's TruSeq RNA Sample Preparation Kit according to manufacturer's instructions. cDNA was prepared using random hexamer priming and Superscript III (Invitrogen), with second strand synthesis using DNA polymerase I and T4 DNA polymerase. cDNA quality was checked at this stage by both Nanodrop spectroscopy and PCR. The resultant cDNA was fragmented using a nebulizer, ends blunted using Klenow and T4 DNA polymerases, adenylated, ligated to Illumina primers, and subjected to limited PCR amplification; 120–170 bp fragments were selected using agarose gel electrophoresis and then sequenced (Wilhelm et al., 2010). These steps were carried out using the Illumina mRNA-Seq 8-Sample Prep Kit. The quality of the libraries was assessed via Bioanalyzer (Agilent), diluted to approximately 10 nM and were combined two-to-three libraries per pool. The pooled libraries were applied to a HiSeq flow cell (version 1.5 flow cell and version 2 cluster generation reagents) at 4 pM resulting in 560–590 clusters/mm$^2$. In our control and *sizzled* morphant study we obtained ~30 million, ~100 base reads per sample. Data was filtered (Wilhelm et al., 2010) to remove uninformative sequences. Quality reads were mapped to the reference genome (*Xenopus tropicalis*, Joint Genome Institute (JGI) assembly version 4.2 from Ensembl) using Bowtie (Langmead et al., 2009) and TopHat (Trapnell et al., 2009). Transcripts were assembled and quantified using Cufflinks (Trapnell et al., 2010).

### *in situ* hybridization and immunoblot studies

For *in situ* hybridization studies, digoxigenin-UTP labeled antisense probes were made following standard methods: specific probes for *brachyury*, *endodermin*, *myoD*, *snail2*, *chd7*, *c-myc*, *sox9*, and *twist1* RNAs were used. Monoclonal anti-tropomyosin was purchased from Sigma and 4A6 (Vize et al., 1995) was a gift from Elizabeth Jones. Whole-mount immunocytochemistry was carried out as described by Dent et al. (Dent et al., 1989), and embryos were cleared with either benzyl alcohol:benzyl benzoate or methyl salicyate. In many cases embryos were co-injected with RNA (50 pg/embryo) encoding β-galactosidase; β-galactosidase activity was visualized in fixed embryos using a brief Red-Gal (Research Organics) reaction, in order to identify successfully injected embryos.

### Quantitative and RT-PCR

RNA isolation, RT-PCR and quantitative RT-PCR analyses were carried out as described previously (Zhang et al., 2003; Zhang et al., 2006). Primers for RT-PCR analyses were *ornithine decarboxylase* (*odc*) [U 5′-CAG CTA GCT GTG GTG TGG-3′ D 5′-CAA CAT GGA AAC TCA CAC-3′]; *sox9* [U 5′-TGC AAT TTT CAA GGC CCT AC –3′ D 5′- GCT GCC TAC CAT TCT CTT GC –3′]; *sizzled* [U 5′-CAT GTC CGG AGT CTT CCT GC –3′ D 5′-GGA TGA ACG TGT CCA GGC AG –3′]; *cerberus* [U 5′-CCT TGC CCT TCA CTC AG –3′ D 5′-TGG CAG ACA GTC CTT T –3′]; *wnt8* [U 5′-TGA TGC CTT CAC TTC TGT GG-3′ D 5′-TCC TGC AGC TTC TTC TCT CC –3′]; *bmp4* [U 5′-TGG TGG ATT AGT CTC GTG TCC –3′ D 5′-TCA ACC TCA GCA GCA TTC C –3′]; *dkk* [U 5′-ACG GAA GAT GAT GAC TGT GC –3′ D 5′-CTC TTG ATC TTG CTC CAC AGG –3′]; *noggin* [U 5′-AGT TGC AGA TGT GGC TCT –3′ D 5′-AGT CCA AGA GTC TCA GCA –3′]; *frzb1* [U 5′- TGG ACT CAT TCC TGC TAC TGG-3′ D 5′-AAT TGC CAG GAT AGC ATT GG –3′]; *sfrp2* [U 5′-TCT GTG TGA GCA GGT GAA GG –3′ D 5′-GTC ATT GTC ATC CTC GTT GC –3′]; *chordin* [U 5′-CCT CCA ATC CAA GAC TCC AGC AG –3′ D 5′-GGA GGA GGA GGA GCT TTG GGA CAA G –3′].

## Acknowledgements

We thank Courtney Severson, Jianxia Yang, and Chi Zhang for their work on the project, Doris Wedlich and Hazel Sive for discussion, and Jim Huntley for RNA SEQ runs. This work was supported by NIH ARRA grant GM84133. We thank the Xenopus community, particularly Eddy DeRobertis and Richard Harland for reagents.

## References

**Akkers, R. C., van Heeringen, S. J., Jacobi, U. G., Janssen-Megens, E. M., Francoijs, K. J., Stunnenberg, H. G. and Veenstra, G. J.** (2009). A hierarchy of H3K4me3 and H3K27me3 acquisition in spatial gene regulation in Xenopus embryos. *Dev. Cell.* **17**, 425-434.

**Alves, C. C., Carneiro, F., Hoefler, H. and Becker, K. F.** (2009). Role of the epithelial-mesenchymal transition regulator Slug in primary human cancers. *Front Biosci.* **14**, 3035-3050.

**Bafico, A., Liu, G., Yaniv, A., Gazit, A. and Aaronson, S. A.** (2001). Novel mechanism of Wnt signalling inhibition mediated by Dickkopf-1 interaction with LRP6/Arrow. *Nat. Cell Biol.* **3**, 683-686.

**Beck, C. W., Sutherland, D. J. and Woodland, H. R.** (1998). Involvement of NF-kappaB associated proteins in FGF-mediated mesoderm induction. *Int. J. Dev. Biol.* **42**, 67-77.

**Bonstein, L., Elias, S. and Frank, D.** (1998). Paraxial-fated mesoderm is required for neural crest induction in Xenopus embryos. *Dev. Biol.* **193**, 156-168.

**Bovolenta, P., Esteve, P., Ruiz, J. M., Cisneros, E. and Lopez-Rios, J.** (2008). Beyond Wnt inhibition: new functions of secreted Frizzled-related proteins in development and disease. *J. Cell Sci.* **121**, 737-746.

**Chaffer, C. L. and Weinberg, R. A.** (2011). A perspective on cancer cell metastasis. *Science* **331**, 1559-1564.

**Collavin, L. and Kirschner, M. W.** (2003). The secreted Frizzled-related protein Sizzled functions as a negative feedback regulator of extreme ventral mesoderm. *Development* **130**, 805-816.

**Dale, L. and Slack, J. M.** (1987). Fate map for the 32-cell stage of Xenopus laevis. *Development* **99**, 527-551.

**De Robertis, E. M.** (2009). Spemann's organizer and the self-regulation of embryonic fields. *Mech. Dev.* **126**, 925-941.

**De Robertis and, E. M. and Kuroda, H.** (2004). Dorsal-ventral patterning and neural induction in Xenopus embryos. *Annu. Rev. Cell Dev. Biol.* **20**, 285-308.

**Dent, J. A., Polson, A. G. and Klymkowsky, M. W.** (1989). A whole-mount immunocytochemical analysis of the expression of the intermediate filament protein vimentin in Xenopus. *Development* **105**, 61-74.

**Esteve, P. and Bovolenta, P.** (2010). The advantages and disadvantages of sfrp1 and sfrp2 expression in pathological events. *Tohoku J. Exp. Med.* **221**, 11-17.

**Glinka, A., Wu, W., Delius, H., Monaghan, A. P., Blumenstock, C. and Niehrs, C.** (1998). Dickkopf-1 is a member of a new family of secreted proteins and functions in head induction. *Nature* **391**, 357-362.

**Hanahan, D. and Weinberg, R. A.** (2011). Hallmarks of cancer: the next generation. *Cell* **144**, 646-674.

**Hausler, K. D., Horwood, N. J., Chuman, Y., Fisher, J. L., Ellis, J., Martin, T. J., Rubin, J. S. and Gillespie, M. T.** (2004). Secreted frizzled-related protein-1 inhibits RANKL-dependent osteoclast formation. *J. Bone Miner. Res.* **19**, 1873-1881.

**Hellsten, U., Harland, R. M., Gilchrist, M. J., Hendrix, D., Jurka, J., Kapitonov, V., Ovcharenko, I., Putnam, N. H., Shu, S., Taher, L. et al.** (2010). The genome of the Western clawed frog *Xenopus tropicalis*. *Science* **328**, 633-636.

**Hugo, H. J., Kokkinos, M. I., Blick, T., Ackland, M. L., Thompson, E. W. and Newgreen, D. F.** (2011). Defining the E-cadherin repressor interactome in epithelial-mesenchymal transition: the PMC42 model as a case study. *Cells Tissues Organs* **193**, 23-40.

**Kennedy, M. W. and Kao, K. R.** (2011). Xrel3/XrelA attenuates beta-catenin-mediated transcription during mesoderm formation in Xenopus embryos. *Biochem. J.* **435**, 247-257.

**Kennedy, M. W., Green, K. A., Ford, R. L., Andrews, P. G., Paterno, G. D., Gillespie, L. L. and Kao, K. R.** (2007). Regulation of the response to Nodal-mediated mesoderm induction by Xrel3. *Dev. Biol.* **311**, 383-395.

**Kielbowna, L.** (1981). The formation of somites and early myotomal myogenesis in Xenopus laevis, Bombina variegata and Pelobates fuscus. *J. Embryol. Exp. Morph.* **64**, 295-304.

**Klymkowsky, M. W. and Hanken, J.** (1991). Whole-mount staining of *Xenopus* and other vertebrates. In *Xenopus laevis: Practical Uses in Cell and Molecular Biology (Methods in Cell Biology)* **36**, (ed.B. K. Kay and H. B. Peng), 419-441. New York: Academic Press.

**Klymkowsky, M. W. and Savagner, P.** (2009). Epithelial-mesenchymal transition: a cancer researcher's conceptual friend and foe. *Am. J. Pathol.* **174**, 1588-1593.

**Kobayashi, K., Luo, M., Zhang, Y., Wilkes, D. C., Ge, G., Grieskamp, T., Yamada, C., Liu, T. C., Huang, G., Basson, C. T. et al.** (2009). Secreted Frizzled-related protein 2 is a procollagen C proteinase enhancer with a role in fibrosis associated with myocardial infarction. *Nat. Cell Biol.* **11**, 46-55.

**Lake, B. B., Ford, R. and Kao, K. R.** (2001). Xrel3 is required for head development in Xenopus laevis. *Development* **128**, 263-273.

**Langmead, B., Trapnell, C., Pop, M. and Salzberg, S. L.** (2009). Ultrafast and memory-efficient alignment of short DNA sequences to the human genome. *Genome Biol.* **10**, R25.

**Lee, H. X., Ambrosio, A. L., Reversade, B. and De Robertis, E. M.** (2006). Embryonic dorsal-ventral signaling: secreted frizzled-related proteins as inhibitors of tolloid proteinases. *Cell* **124**, 147-159.

**Micalizzi, D. S., Farabaugh, S. M. and Ford, H. L.** (2010). Epithelial-mesenchymal transition in cancer: parallels between normal development and tumor progression. *J Mammary Gland Biol. Neoplasia* **15**, 117-134.

**Mii, Y. and Taira, M.** (2009). Secreted Frizzled-related proteins enhance the diffusion of Wnt ligands and expand their signalling range. *Development* **136**, 4083-4088.

**Misra, K. and Matise, M. P.** (2010). A critical role for sFRP proteins in maintaining caudal neural tube closure in mice via inhibition of BMP signaling. *Dev. Biol.* **337**, 74-83.

**Moody, S. A.** (1987). Fates of the blastomeres of the 32-cell-stage Xenopus embryo. *Dev. Biol.* **122**, 300-319.

**Muntz, L.** (1975). Myogenesis in the trunk and leg during development of the tadpole of *Xenopus laevis* (Daudin 1802). *J. Embryol. Exp. Morphol.* **33**, 757-774.

**Muraoka, O., Shimizu, T., Yabe, T., Nojima, H., Bae, Y. K., Hashimoto, H. and Hibi, M.** (2006). Sizzled controls dorso-ventral polarity by repressing cleavage of the Chordin protein. *Nat. Cell Biol.* **8**, 329-338.

**Nakamura, O., Takasaki, H. and Nagata, A.** (1978). Further studies of the prospective fates of blastomeres at the 32-cell stage of Xenopus laevis embryos. *Med. Biol.* **56**, 355-360.

**Nieuwkoop, P. D. and Faber, J.** (1994). Normal table of Xenopus laevis (Daudin): A Systematical and Chronological Survey of the Development from the Fertilized Egg till the end of Metamorphosis. New York: Garland Publishing.

**Ploper, D., Lee, H. X. and De Robertis, E. M.** (2011). Dorsal-ventral patterning: Crescent is a dorsally secreted Frizzled-related protein that competitively inhibits Tolloid proteases. *Dev. Biol.* **352**, 317-328.

**Rubenstein, A., Merriam, J. and Klymkowsky, M. W.** (1997). Localizing the adhesive and signaling functions of plakoglobin. *Dev. Genet*. **20**, 91-102.

**Salic, A. N., Kroll, K. L., Evans, L. M. and Kirschner, M. W.** (1997). Sizzled: a secreted Xwnt8 antagonist expressed in the ventral marginal zone of Xenopus embryos. *Development* **124**, 4739-4748.

**Schier, A. F.** (2009). Nodal morphogens. *Cold Spring Harb. Perspect. Biol*. **1**, a003459.

**Semenov, M. V., Tamai, K., Brott, B. K., Kuhl, M., Sokol, S. and He, X.** (2001). Head inducer Dickkopf-1 is a ligand for Wnt coreceptor LRP6. *Curr. Biol.* **11**, 951-961.

**Shi, J., Severson, C., Yang, J., Wedlich, D. and Klymkowsky, M. W.** (2011). Snail2 controls BMP- and Wnt-dependent mesodermal induction of neural crest. *Development* **138**, 3135-3145.

**Shirley, S. H., Hudson, L. G., He, J. and Kusewitt, D. F.** (2010). The skinny on Slug. *Mol. Carcinog*. **49**, 851-861.

**Sive, H. L., Grainger, R. M. and Harland, R. M.** (2000). Early Development of Xenopus Laevis: a Laboratory Manual. Cold Spring Harbor: Cold Spring Harbor Laboratory Press.

**Smith, J. C.** (2009). Forming and interpreting gradients in the early Xenopus embryo. *Cold Spring Harb. Perspect. Biol.* **1**, a002477.

**Smith, W. C. and Harland, R. M.** (1992). Expression cloning of noggin, a new dorsalizing factor localized to the Spemann organizer in Xenopus embryos. *Cell* **70**, 829-840.

**Tannahill, D. and Wardle, F. C.** (1995). Control of axis formation in Xenopus by the NF-kappa B-I kappa B system. *Int. J. Dev. Biol.* **39**, 549-558.

**Trapnell, C., Pachter, L. and Salzberg, S. L.** (2009). TopHat: discovering splice junctions with RNA-Seq. *Bioinformatics* **25**, 1105-1111.

**Trapnell, C., Williams, B. A., Pertea, G., Mortazavi, A., Kwan, G., van Baren, M. J., Salzberg, S. L., Wold, B. J. and Pachter, L.** (2010). Transcript assembly and quantification by RNA-Seq reveals unannotated transcripts and isoform switching during cell differentiation. *Nat. Biotechnol.* **28**, 511-515.

**Vize, P. D., Jones, E. A. and Pfister, R.** (1995). Development of the Xenopus pronephric system. *Dev. Biol.* **171**, 531-540.

**Wessely, O. and Tran, U.** (2011). Xenopus pronephros development-past, present, and future. *Pediatr. Nephrol.* **26**, 1545-1551.

**Wilhelm, B. T., Marguerat, S., Goodhead, I. and Bahler, J.** (2010). Defining transcribed regions using RNA-seq. *Nat. Protoc.* **5**, 255-266.

**Yabe, T., Shimizu, T., Muraoka, O., Bae, Y. K., Hirata, T., Nojima, H., Kawakami, A., Hirano, T. and Hibi, M.** (2003). Ogon/Secreted Frizzled functions as a negative feedback regulator of Bmp signaling. *Development* **130**, 2705-2716.

**Zhang, C. and Klymkowsky, M. W.** (2009). Unexpected functional redundancy between Twist and Slug (Snail2) and their feedback regulation of NF-kappaB via Nodal and Cerberus. *Dev. Biol.* **331**, 340-349.

**Zhang, C., Basta, T., Jensen, E. D. and Klymkowsky, M. W.** (2003). The beta-catenin/VegT-regulated early zygotic gene Xnr5 is a direct target of SOX3 regulation. *Development* **130**, 5609-5624.

**Zhang, C., Carl, T. F., Trudeau, E. D., Simmet, T. and Klymkowsky, M. W.** (2006). An NF-kappaB and slug regulatory loop active in early vertebrate mesoderm. *PLoS ONE* **1**, e106.